Supplementary Information (SI) for Journal of Materials Chemistry B.
This journal is © The Royal Society of Chemistry 2025

Supporting Information

Dual-Driven Biodegradable Nanomotors for Enhanced Cellular Uptake

Jianhong Wang[a], Andreas Polyviou[a], Jari F. Scheerstra[a], Shoupeng Cao[b], Alexander D. Fusi[a], Jingxin Shao[a, *], and Jan C. M. van Hest[a, *]

[a] Bio-Organic Chemistry, Departments of Biomedical Engineering and Chemical Engineering & Chemistry, Institute for Complex Molecular Systems, Eindhoven University of Technology, 5600 MB Eindhoven, The Netherlands;

[b] College of Polymer Science and Engineering, State Key Laboratory of Polymer Materials Engineering, Sichuan University, Chengdu 610065, P. R. China.

Keywords: Biodegradable stomatocytes; platinum nanoparticles; autonomous movement; dual driving force; intracellular transport

---

*Corresponding author.

E-mail: J.Shao@tue.nl (J. Shao), J.C.M.v.Hest@tue.nl (J. van Hest)

Experimental section

1.1 Materials

All compounds were purchased from Sigma-Aldrich and used without further purification unless otherwise specified. Poly(ethylene glycol) methyl ether with molecular weights of 1K and 2K was obtained from Rapp Polymers and freeze-dried prior to use. D,L-lactide (DLL) was sourced from Acros Organics. 1,4-Dioxane, toluene, dichloromethane (DCM), and tetrahydrofuran (THF) were supplied by Biosolve Chimie. Chlorin e6 (Ce6) was acquired from Frontier Scientific. Dialysis membranes, with a molecular weight cutoff (MWCO) of 12,000 - 14,000 Da, were provided by Spectra/Pro®. Glucose oxidase (E.C. 1.1.3.4) (GOx) from *Aspergillus niger,* type II, lyophilized powder (100000-250000 U mg^{-1}), genipin (≥98% purity by HPLC), glucose, and hydrogen peroxide (H_2O_2) were obtained from Sigma-Aldrich.

1.2 Instruments

1.2.1 Nuclear Magnetic Resonance Spectroscopy (^{1}H NMR): Routine proton nuclear magnetic resonance (^{1}H NMR) measurements were recorded on a Bruker AV 400 MHz UltrashieldTM spectrometer, $CDCl_3$ was selected as the solvent and tetramethylsilane (TMS) as the internal standard for ^{1}H NMR.

1.2.2 Gel Permeation Chromatography (GPC): The molecular weights (Mw, Mn) and dispersity index (Đ) of the block copolymers were measured using a Prominence-I GPC system (Shimadzu) with a PL gel 5 µm mixed D (Polymer Laboratories), equipped with a RID-20A differential refractive index detector. Polystyrene standards were used for calibration. THF was used as eluent, with a flow rate of 1 mL min^{-1}.

1.2.3 Dynamic Light scattering (DLS): The zeta potential, hydrodynamic size, and polydispersity index (PDI) of the nanoparticles were measured using a Malvern instruments Zetasizer Nano ZSP, equipped with a 633 nm He-Ne laser and an avalanche photodiode detector. Data analysis was conducted with Zetasizer software.

1.2.4 UV-Vis spectroscopy: UV-Vis absorbance measurements were conducted using a UV-Vis spectrophotometer (V-650, JASCO) using a 1 mL black quartz cuvette.

1.2.5 Microplate Reader: Microplate readers Safire^2 and Spark ® 10M (both TECAN) were used in this study.

1.2.6 Infrared camera: Infrared thermal images of the solution (500 µL in a 1.5

mL Eppendorf tube) during irradiation were captured using a compact thermal imaging camera (FLIR E54) and quantified with FLIR Tools software.

1.2.7 Thermometer: Temperature profiles of the solutions (500 µL in a 1.5 mL Eppendorf tube) during irradiation were measured using a thermometer (Chauvin Arnoux, C.A 1823).

1.2.8 Cryogenic transmission electron microscopy (cryo-TEM): Cryo-TEM was conducted on a TU/e Glacios (Thermo Fisher Scientific) equipped with a Falcon 4i direct electron detector, an autoloader station, and a post-column Gatan energy filter. TEM grids (R2/2, Cu, Quantifoil Jena grids, Quantifoil Micro Tools GmbH) were first plasma-treated in a Cressington 208 carbon coater for 40 seconds prior to use. A 3 µL nanoparticle solution was then pipetted onto the grid and blotted using a Vitrobot MARK IV (Thermo Fisher Scientific) at 100% humidity. The grid was blotted for 3.5 seconds (blotting force: −3) before being immediately plunged and frozen in liquid ethane.

1.2.9 Scanning electron microscopy (SEM): The morphology of polymersomes and stomatocytes were characterized by SEM (FEI Quanta 200 3D FEG) at 5.00 kV voltage.

1.2.10 NanoSight Tracking Analysis (NTA): Single particle tracking analysis was conducted using a Nanosight NS300, equipped with a 488 nm laser channel and an sCMOS camera.

1.2.11 Movement analysis: By tracking the X and Y coordinates of at least 20 particles, the mean square displacement (MSD) of the nanomotors was calculated following established methods[1-3]. MSD curves were derived from NTA-recorded trajectories using the following equation,

$$\text{MSD} = \left[\Delta r^2(t)\right] = \left[\frac{1}{N}\sum_{i=0}^{N}\left(r_i(t) - r_i(0)\right)^2\right]$$

where r = radius, t = sampling time, and MSD(t) = 2dD. Here D = diffusion coefficient and d = dimensionality (NTA measurements have dimension d = 2). The equation MSD = $(4D)\Delta t + (v^2)(\Delta t^2)$ was used to fit the MSD curves. From the fitting of these curves, the average particle velocity was determined. According to the particle diffusion coefficient, as described by Golestanian's diffusiophoretic model, a particle undergoing Brownian motion exhibits a linear MSD fitting line over time, with the slope determined by the diffusion coefficient given by $D = KBT / (6\pi\eta R)$. If the particles are in Brownian motion, the linear component of the MSD can be extracted from the equation MSD = $(4D)\Delta t$.

2 Methods

2.1 Synthesis of block copolymers

The PEG-PDLLA copolymers were synthesized via ring-opening polymerization (ROP), following established protocols (**Scheme S1**)[4, 5]. Briefly, the macroinitiator monomethoxy-poly(ethylene glycol)-OH (1K and 2K) and D,L-lactide (DLL) were weighed into a round-bottom flask (100 mL) equipped with a stirring bar. Specifically, for PEG_{22}-$PDLLA_{95}$, 200 mg of PEG 1K and 2.736 g of DLL were used, while for PEG_{44}-$PDLLA_{95}$, 200 mg of PEG 2K and 1.368 g of DLL were employed. The compounds were dried by dissolving them in dry toluene (50 mL, twice), followed by evaporation. The dried compounds were then co-dissolved in dry dichloromethane (DCM) ([monomer] = 0.5 M) under an argon atmosphere. Next, 1,8-diazabicyclo[5.4.0]undec-7-ene (DBU) (0.5 equivalents relative to the initiator; 0.1 mmol = 15 µL) was added to the reaction mixture. The reaction was stirred for 2 - 4 hours at room temperature (RT) under argon, and the progress was monitored by ^{1}H NMR spectroscopy until the peaks corresponding to the monomer had disappeared. Upon completion of the polymerization, the reaction mixture was diluted with DCM and extracted with 1 M $KHSO_4$ (2 times) and brine (1 time). The organic layer (lower layer) was collected, dried over Na_2SO_4, filtered, and concentrated. Precipitation of the concentrated solution was then performed in ice-cold diethyl ether (100 mL), and the precipitate was collected via centrifugation (4350 rpm, 7 min) and lyophilization from 1,4 dioxane (10 mL) to yield a white powder (yield = 80 - 85%). The polymerization was analyzed using ^{1}H NMR spectroscopy (**Figure S5.1**) and GPC (**Table S5.1**). ^{1}H NMR (Chloroform-d): 5.15-5.3 ppm (-C=OCHCH$_3$-, 2H, multiplet), 3.63-3.7 ppm (-CH$_2$CH$_2$O-, 4H PEG, multiplet), 3.35-3.40 ppm (CH$_3$-PEG, singlet) and 1.55-1.65 ppm (C=OCHCH$_3$-, 6H, multiplet).

2.2 Preparation of stomatocytes

In a 20 mL vial, PEG_{22}-$PDLLA_{95}$ and PEG_{44}-$PDLLA_{95}$ copolymers (1:1 w/w, 10 mg) were weighed and dissolved in 1 mL of a THF and dioxane mixture (1:4 v/v). A stirring bar was then added, and the vial was sealed with a rubber septum. The solution was stirred at 900 rpm for 30 minutes, after which 2 mL of Milli-Q water was added using a syringe pump (Chemyx Inc. Fusion 100 Syringe Pump) at a rate of 1 mL h^{-1}. The resulting cloudy suspension was transferred into a pre-hydrated dialysis membrane (SpectraPor, molecular weight cut-off: 12-14 kDa, 2 mL cm^{-1}) and dialyzed at 4 °C against pre-cooled NaCl solution (50 mM, 2 L) for at least 24 h, with a NaCl solution change after

1 h to yield stomatocytes. For comparison, polymersomes were prepared by dialysis against Milli-Q water for at least 24 h, with a water change after 1 h at 4 °C. For Ce6 loading, 0.4 mg of Ce6 was dissolved together with the block copolymers prior to self-assembly.

2.3 Encapsulation of GOx

After obtaining the stomatocytes, 1 mg of GOx was mixed with 1 mL of the stomatocytes solution (3.33 mg mL^{-1}) and stirred vigorously at room temperature (RT) for 8 hours. The free GOx was then removed by centrifugation (10000 rpm, 10 min). Next, 1 mL of a genipin solution (50 mM) was added to 100 µL of stomatocyte sample, and the reaction mixture was gently stirred for 24 h at RT. After 24 h, genipin was removed from the solution using centrifugation (10 kDa filters, 10000 rpm, 10 min).

2.4 Preparation of Pt-stomatocytes and Pt-polymersomes

For the preparation of Pt-stomatocytes, platinum nanoparticles were synthesized using the *in situ* growth method and displayed onto the surface of the stomatocytes through non-covalent interactions, following a previously reported protocol[3]. In a 4 mL vial, poly(acrylic acid) (PAA, 0.8 mg) and $H_2PtCl_6.6H_2O$ (1.2 µL, 0.5 M) were added to 1 mL of the stomatocyte solution (3.33 mg mL^{-1}). The mixture was stirred at 200 rpm for 10 minutes at RT. Next, a $NaBH_4$ solution (1 mL, 5 mM) was added dropwise, and the mixture was stirred for an additional 5 minutes at RT. The solution was then centrifuged at 7000 rpm for 10 minutes; the supernatant was discarded, and Milli-Q water was added. This washing procedure was repeated until the supernatant was clear. Finally, the precipitate was dispersed in 1 mL of Milli-Q water to achieve a stomatocyte concentration of 3.33 mg mL^{-1}. Samples were stored in the refrigerator prior to further use. Pt-polymersomes, serving as a control group, were prepared using the same procedure.

2.5 Preparation of GOx-loaded Pt-stomatocytes

Following the aforementioned procedures, the obtained GOx-loaded stomatocytes were mixed with PAA and $H_2PtCl_6.6H_2O$ and stirred at 200 rpm for 10 minutes at RT. Subsequently, a $NaBH_4$ solution (1 mL, 5 mM) was added dropwise, and the mixture was stirred for an additional 5 minutes at RT. The solution was then centrifuged at 7000 rpm for 10 minutes; the supernatant was removed, and Milli-Q water was added. This washing procedure was repeated until the supernatant was clear. Finally, the precipitate was dispersed in 1 mL of Milli-Q water to achieve a stomatocyte concentration of 3.33 mg mL^{-1}. The

resulting GOx-Pt-stomatocytes were stored in the fridge prior to further use. For the preparation of Ce6/GOx-Pt-stomatocytes, the Ce6 loaded stomatocytes were used in place of the stomatocytes.

2.6 Measurement of concentration of GOx

The measurement of glucose oxidase (GOx) activity involved the preparation of a standard curve (y = 4678x+3648.8) using a GOx stock solution to achieve concentrations ranging from 0 to 10 mU mL^{-1} in a volume of 50 µL. The GOx-stomatocytes were similarly diluted to identify the optimal sample amount within the standard curve range. Both the standard curve and experimental samples were placed into separate wells of a microplate. The reaction was initiated by adding 50 µL of a working solution containing D-glucose (1.25 mL of 400 mM, 100 mM), HRP (100 µL of 10 U ml^{-1}, 0.2 U mL^{-1}), and Ampliflu™ Red (50 µL of 10 mM in DMSO, 100 µM) to each well using a multi-pipette. The progression of the reaction was observed directly over 10 minutes by measuring the increase in fluorescence emission at 590 nm after excitation at 550 nm. Finally, to correct for background fluorescence, the value from a no-GOx control was subtracted from each data point. For GOx, a linear trend fit (**Figure S11**) was applied to measure solutions containing unknown amounts of the enzyme in order to determine the quantity of active enzyme present.

2.7 Photothermal performance of Pt-stomatocytes

0.5 mL samples were transferred into 1.5 mL Eppendorf tubes and irradiated with an external NIR laser (808 nm) for 600 s. The temperature was recorded every second using a digital thermometer equipped with a thermocouple probe. Additionally, IR images of the sample solutions were captured using a thermal imaging camera (FLIR E54).

2.8 Photothermal conversion efficiency

The photothermal conversion efficiency (η) of the Pt-stomatocytes was calculated according to the published method[6]. The calculations were performed according to the following equations:

$$t = -\tau s \ln\theta = -\tau s \ln\frac{T - Tsurr}{Tmax - Tsurr} \qquad (1)$$

$$hA = \frac{mCwater}{\tau s} \quad (2)$$

$$Qdis = \frac{mCwater\ (Tmax(water)\ -\ Tsurr)}{\tau water} \quad (3)$$

$$\eta = \frac{hA(Tmax - Tsurr) - Qdis}{I(1 - 10 - A808)} \quad (4)$$

Where T_{surr} is the surrounding temperature, T_{max} and $T_{max(water)}$ represent the maximum temperature of the Pt-stomatocyte solution and water, respectively. τs (**Figure S5**) and $\tau water$ (**Figure S6**) represent the system time constants of 206 s and 275 s, respectively. h is the heat transfer coefficient. A represents the surface area of the container, m represents the mass of the solution (m = 0.5 g), and C_{water} = 4.2 J g•℃$^{-1}$. Q_{dis} is measured to be 0.013 W, I signifies the incident laser power (1 W cm^{-2}), and A_{808} represents the absorbance of the Pt-stomatocyte solution (A_{808} = 0.415). The photothermal conversion efficiency (PCE), denoted as η, was calculated to be 30% for the Pt-stomatocytes.

2.9 Motility studies

The autonomous motion of Pt-stomatocytes and control nanoparticles was measured using nanoparticle tracking analysis (NTA) with an external 808 nm laser (UltraLasers). 1.2 µL samples (3.33 mg mL^{-1}) were suspended in 1 mL of Milli-Q water and loaded into the NTA chamber using a syringe. The movement of the nanoparticles was recorded for 30 s. NTA 2.2 software was then employed to track and analyze the trajectories of individual nanoparticles.

2.10 In vitro experiments

2.10.1 Cell culture

Human cervical cancer cells (HeLa) were cultured in DMEM medium supplemented with 10% fetal bovine serum (FBS) and 1% 100 U mL^{-1} penicillin & streptomycin in the cell incubator (ThermoFisher) under an atmosphere of 5% CO_2 at 37 °C and 70% humidity.

2.10.2 Cell viability of GOx-Pt-stomatocytes

In vitro cytotoxicity of the GOx-Pt-stomatocytes was measured using a standard CCK-8 assay with a microplate reader (Safire^2, TECAN). For the biocompatibility assessment, cells were seeded in 96-well plates at a density of 1×10^4 cells per well in 100 µL of DMEM supplemented with FBS, penicillin and

streptomycin. The cells were incubated overnight. The medium in each well was then refreshed with medium containing stomatocytes and GOx-Pt-stomatocytes at different concentrations (0, 40, 80, 100, 200, and 400 μg mL^{-1}). After 24 h of incubation, the cells were washed three times with PBS and treated with 100 μL of DMEM containing 10% CCK-8 for 3 h. The absorbance of each well was recorded at 450 nm using the microplate reader. For each group, triplicate wells were tested, and the data were presented as mean ± SD.

2.10.3 Intracellular uptake of Ce6/GOx-loaded Pt-stomatocyte nanomotors (Ce6/GOx-Pt-stomatocytes)

To evaluate intracellular uptake behavior, HeLa cells were cultured in μ-Slide 8 well plates at a density of 2×10^4 cells per well in 200 μL of DMEM. The cell nucleus and membrane were stained with Hoechst 33342 and Alexa Fluor™ 488. The HeLa cells were then mixed with Ce6/GOx-Pt-stomatocytes (20 μL) and treated with an external 808 nm laser at an output laser power (1 W) for 5 min. Afterward, the cells were co-cultured for an additional 6 hours and subsequently washed three times with PBS. Confocal microscopy was then performed to image the cells.

2.10.4 Cell uptake of Ce6/GOx-Pt-stomatocytes in HeLa cells

The pre-seeded HeLa cells were mixed with Ce6/GOx-Pt-stomatocytes and treated with an external 660 nm laser at different output laser power (0 or 1 W) for 5 min. After co-culturing for an additional 6 hours, the cells were washed three times with PBS. HeLa cells were then stained with Hoechst 33342 to visualize the cell nucleus. Confocal laser scanning microscopy (CLSM) was subsequently performed to image the cells.

2.10.5 Flow cytometry

To quantitatively confirm the cellular uptake of Ce6 within HeLa cells, the Ce6 fluorescence within the cells was monitored using a BD FACSymphony A3 Cell Analyzer (BD Biosciences). HeLa cells were seeded into a 12-well tissue culture plate (2×10^5 cells per well) for 24 h. Then, the cell medium of each well was replaced with fresh DMEM containing the Ce6-stomatocytes (treated with laser, 660 nm, 1 W, 5 min), Ce6-Pt-stomatocytes (treated with laser, 660 nm, 1 W, 5 min), Ce6/GOx-Pt-stomatocytes, and Ce6/GOx-Pt-stomatocytes (treated with laser, 660 nm, 1 W, 5 min) and the cells were incubated for 8 h under regular culture conditions. After that, the medium in each well was discarded and the cells were washed with PBS for 3 times, trypsinized, centrifuged, and resuspended in 1 mL of PBS supplemented with 0.5% BSA and 2 mM EDTA before flow cytometry analysis. For each sample, at least 1×10^4 cells were recorder, and each measurement was repeated 3 times. Cells treated with PBS were used as negative control. Data was analyzed using FlowJo 10.9.0

software (Tree Star) to obtain Ce6 geometric mean fluorescence intensity valuses.

3. Supplementary Figures and Tables

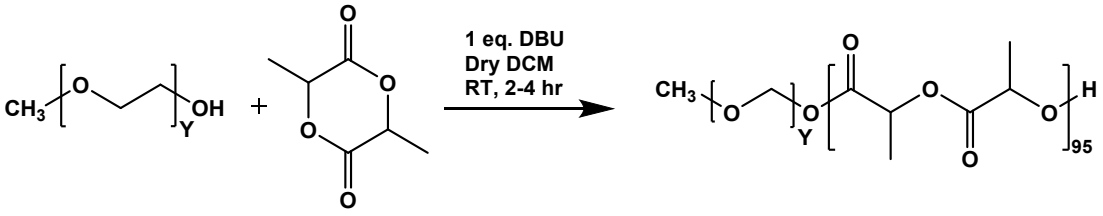

$PEG_{22/44}$ **DLL** **$PEG_{22/44}$-$PDLLA_{95}$**

Y = 22 or 44

Scheme 1. Synthetic route for the preparation of $PEG_{22/44}$-$PDLLA_{95}$ block polymers.

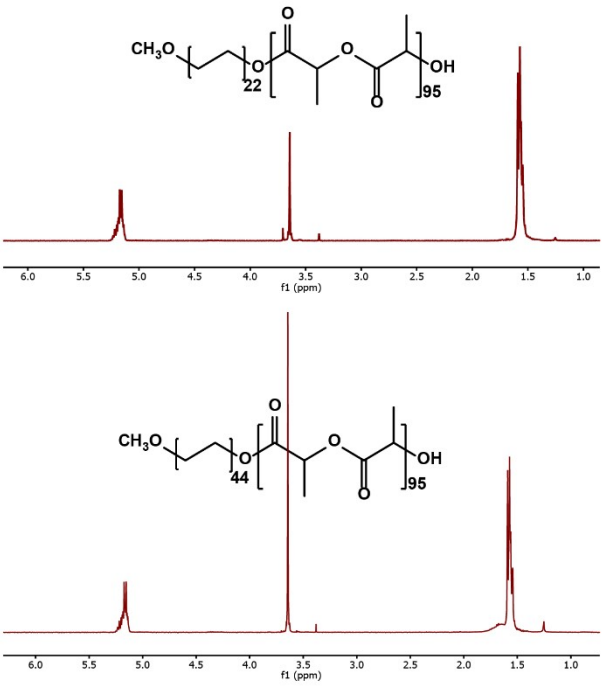

Figure S1. Characterization of PEG-PDLLA copolymers with ^{1}H NMR spectroscopy.

Table S1. Overview of PEG-PDLLA block copolymer compositions. The degree of polymerization (DP) of the copolymers was calculated by integrating the characteristic proton peaks in the ^{1}H NMR spectra.

Sample	DP (NMR)	M_W/kDa (GPC)	Đ (GPC)
PEG_{22}-$PDLLA_{95}$	91	11.3	1.08
PEG_{44}-$PDLLA_{95}$	96	14.1	1.08

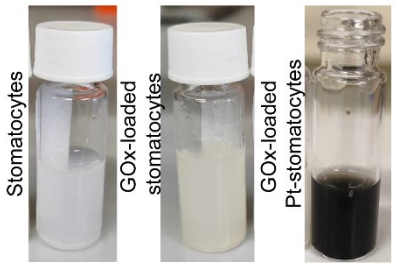

Figure S2. Photographs of stomatocytes, GOx-loaded stomatocytes, and GOx-loaded Pt-stomatocytes in Milli-Q water.

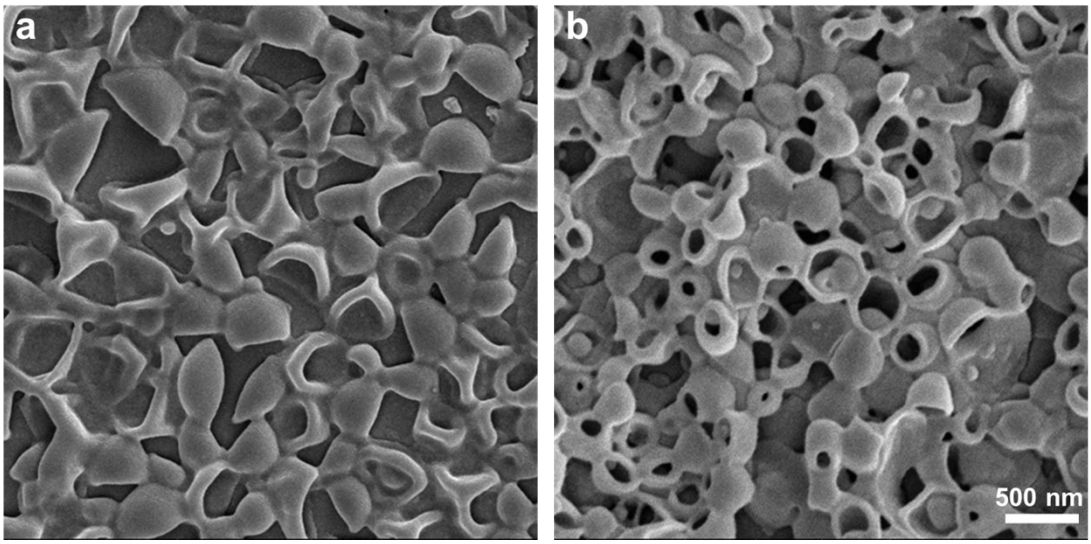

Figure S3. SEM morphological characterization of polymersomes (a) and stomatocytes (b). Scale bar = 500 nm.

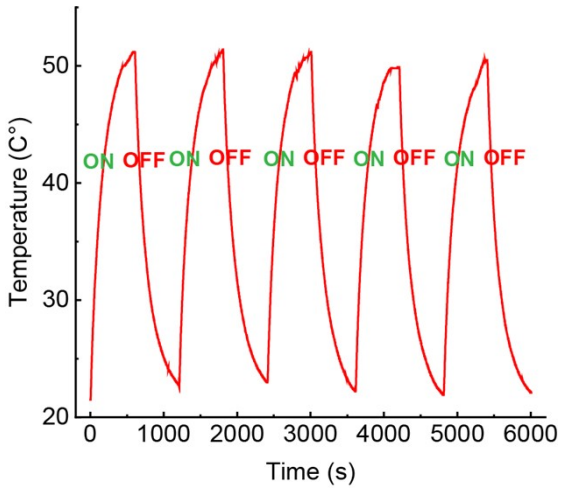

Figure S4. Photothermal stability of Pt-stomatocytes (3.33 mg mL-1) in aqueous solution under cyclic laser irradiation (808 nm, 1.2 W).

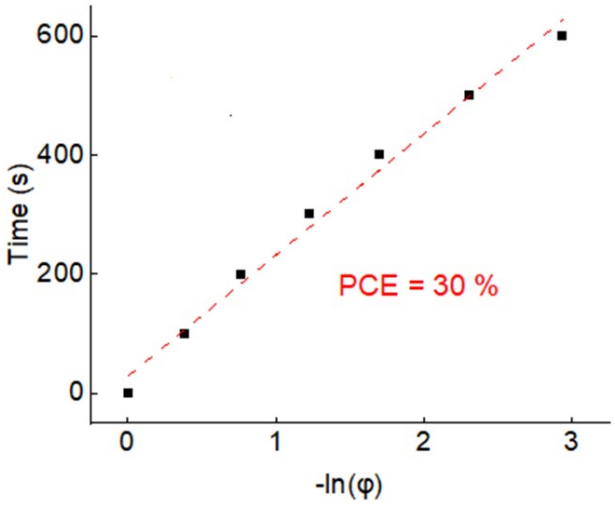

Figure S5. The time constant of Pt-stomatocytes heat transfer in water was obtained from the linear time data (0, 100, 200, 300, 400, 500, and 600 s) during the cooling period versus the negative natural logarithm of the driving force temperature. The photothermal conversion efficiency (PCE) was calculated to be 30%.

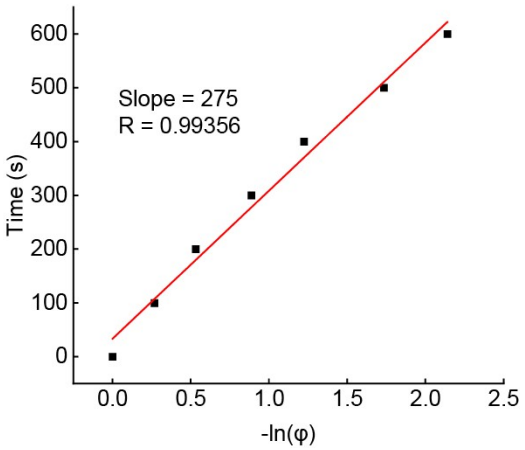

Figure S6. The time constant of water heat transfer was obtained from linear time data (0, 100, 200, 300, 400, 500, and 600 s) during the cooling period.

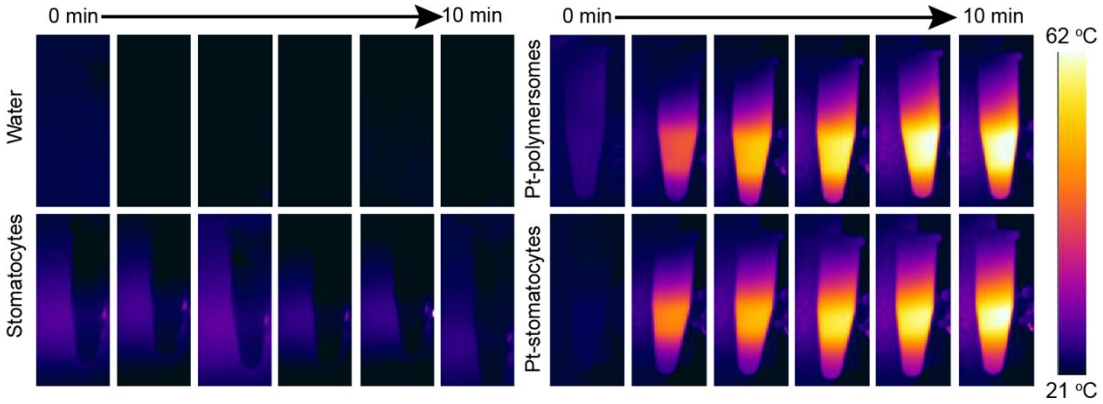

Figure S7. Infrared thermographic maps of aqueous samples containing Pt-stomatocytes, stomatocytes, Milli-Q water, and Pt-polymersomes at a concentration of 3.33 mg mL^{-1} were obtained as a function of irradiation time under 808 nm light at an intensity of 1.2 W.

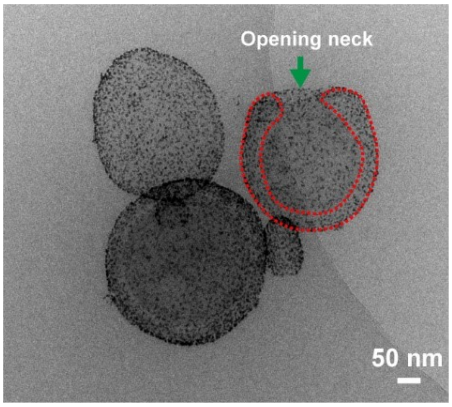

Figure S8. Cryo-TEM images of Pt-stomatocytes after irradiation with an 808 nm laser (1.2 W) for 10 min.

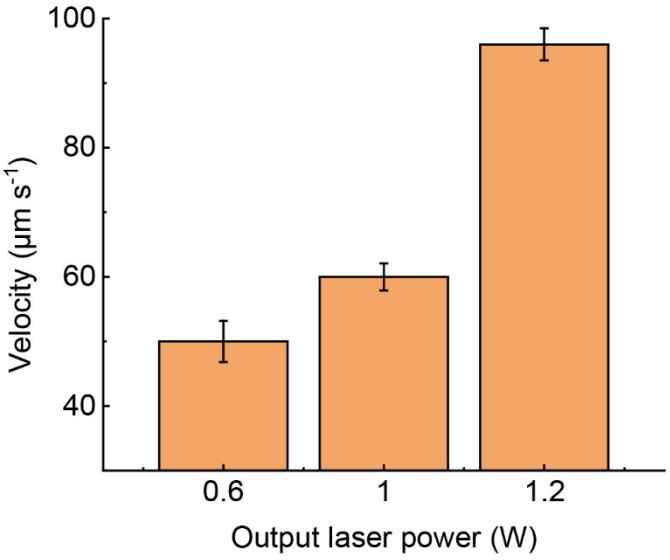

Figure S9. Velocities of Pt-stomatocytes as a function of output laser power.

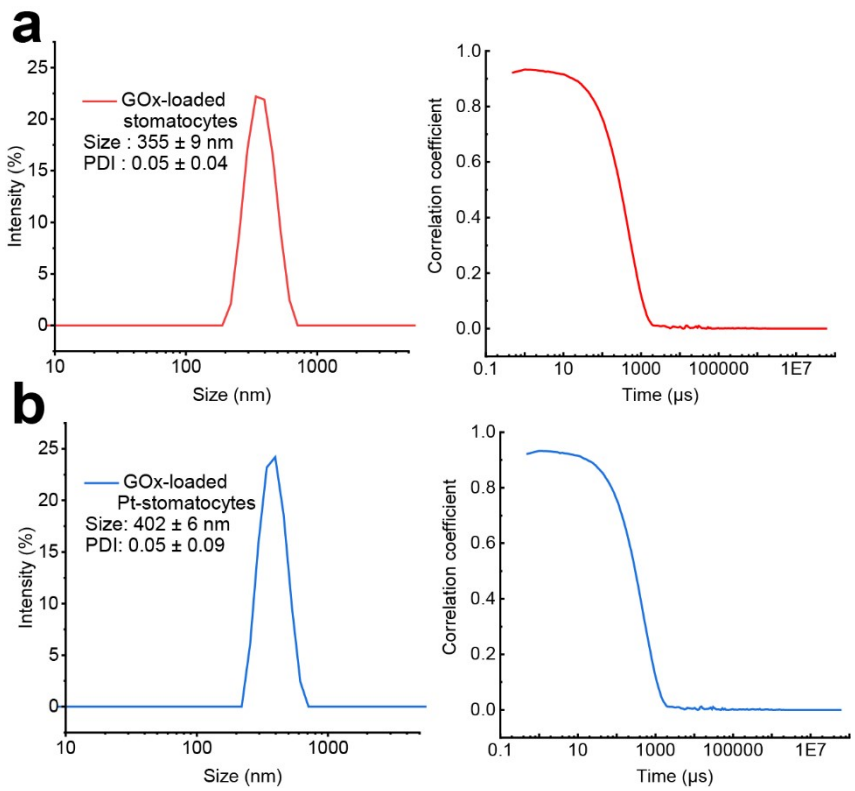

Figure S10. a) Hydrodynamic size and PDI (left), as well as correlation coefficient (right) of GOx-loaded stomatocytes. **b)** Hydrodynamic size and PDI (left), as well as correlation coefficient (right) of GOx-Pt-stomatocytes measured by DLS.

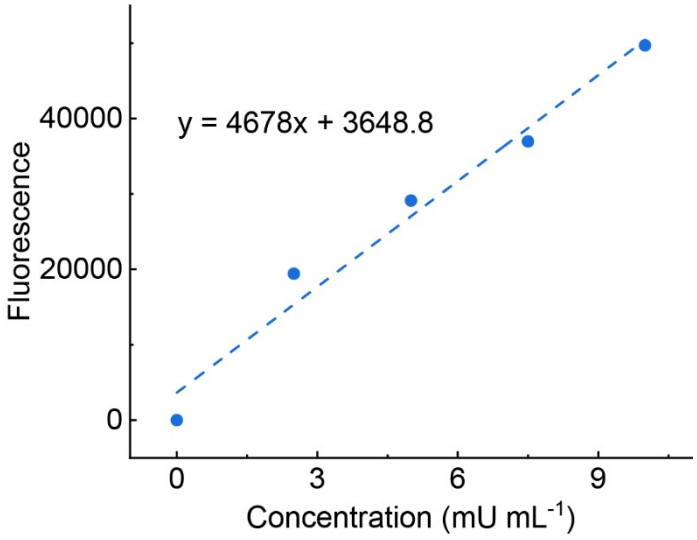

Figure S11. Calibration curve of free glucose oxidase with the concentrations ranging from 0 to 10 mU mL^{-1}.

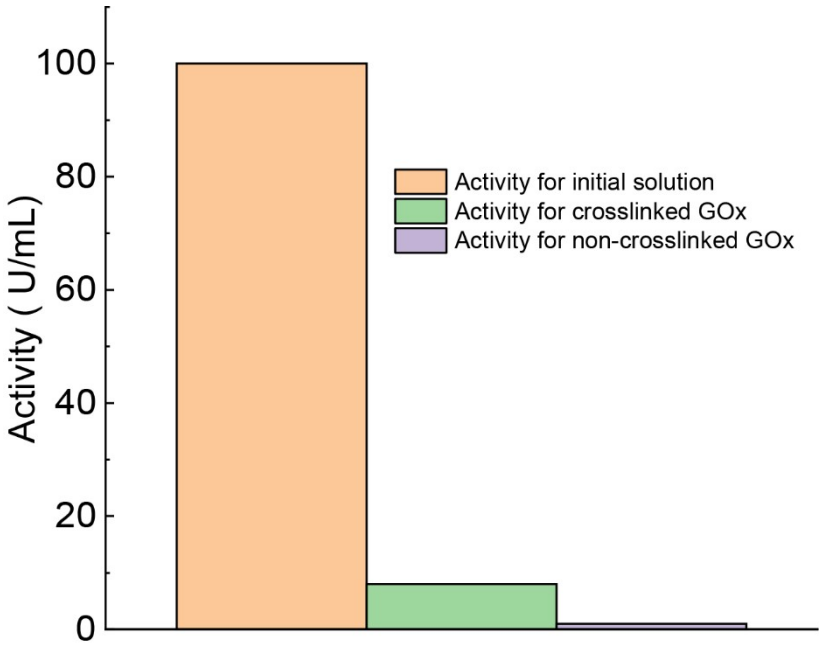

Figure S12. Quantification of GOx activity of the original enzyme solution used for the encapsulation experiment, encapsulated and crosslinked enzyme in stomatocytes, and encapsulated uncrosslinked enzyme in stomatocytes.

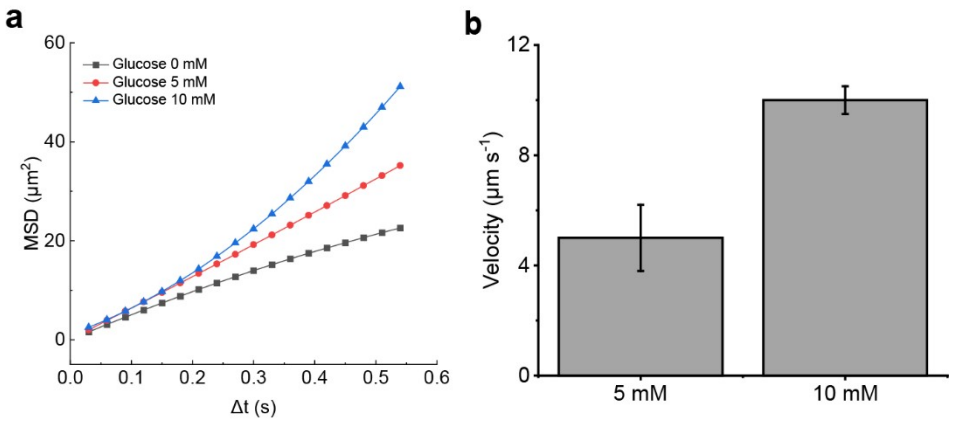

Figure S13. Mean square displacements (MSDs) a) of GOx-Pt-stomatocytes in the presence of glucose (0, 5, and 10 mM). b) Velocity of GOx-Pt-stomatocytes in the presence of glucose (5 and 10 mM).

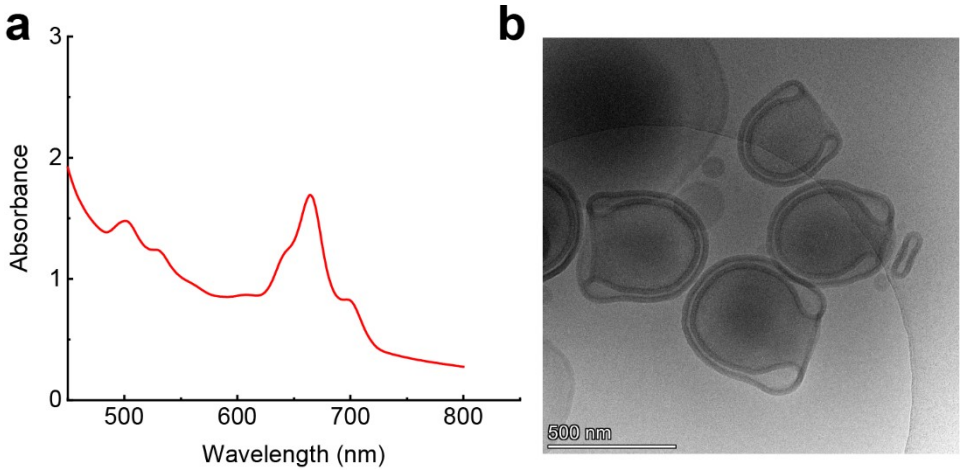

Figure S14. a) UV-Vis spectrum and b) cryo-TEM image of Ce6-loaded stomatocytes.

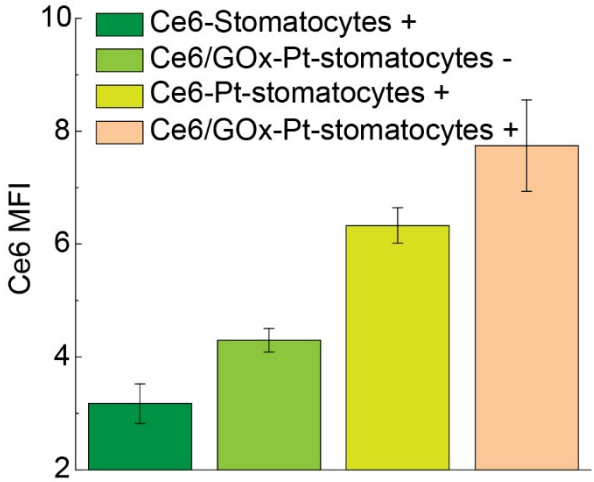

Figure S15. Fluorescence intensity of Ce6 signals in HeLa cells (**Figure 5c**) analyzed using ImageJ.

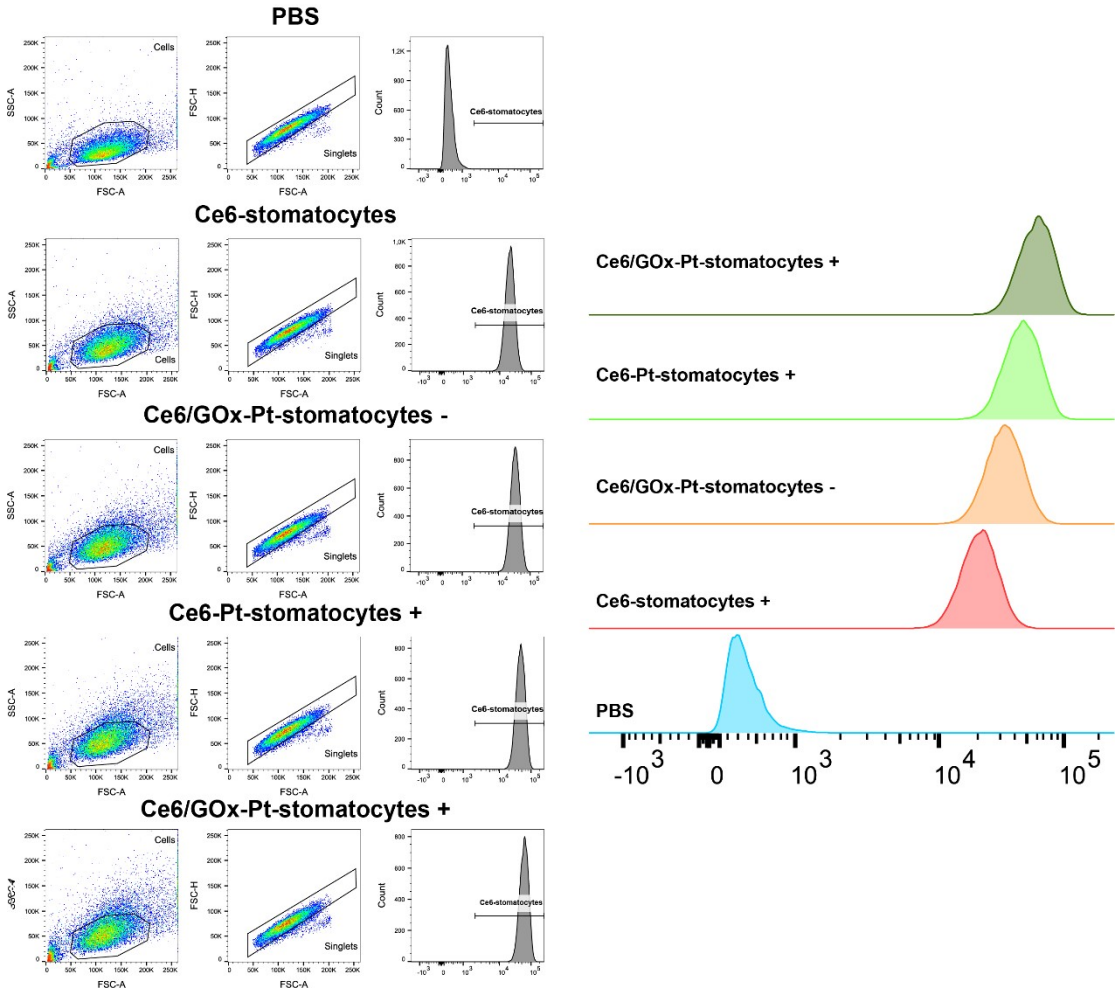

Figure S16. Flow cytometric analysis of HeLa cells after treatment with Ce6-stomatocytes (with laser irradiation, 808 nm, 1 W, 5 min) and Ce6/GOx-Pt-stomatocytes (without or with laser irradiation, 808 nm, 1 W, 5 min) after incubation with HeLa cells for 8 h.

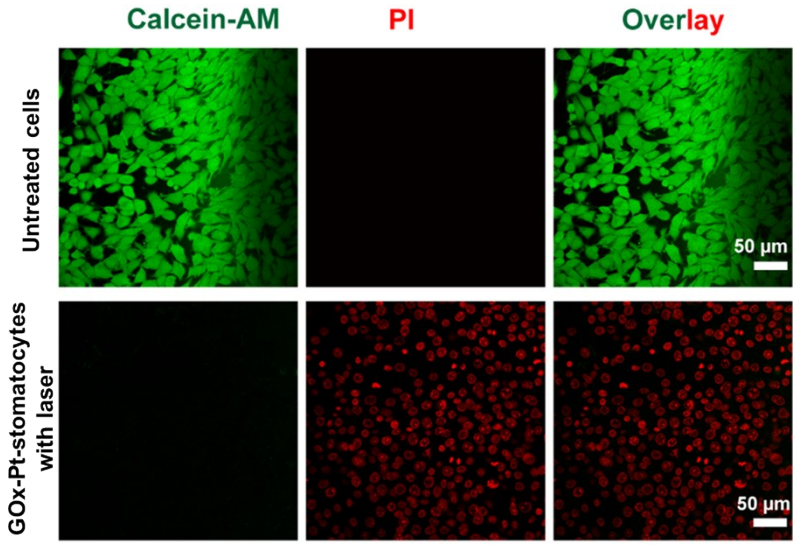

Figure S17. CLSM images show HeLa cells after treatment with different groups: untreated cells and cells treated with GOx-Pt-stomatocytes and laser irradiation (808 nm, 1 W, 5 min)). Live cells are indicated by a green signal (Calcein-AM staining), while dead cells are marked by a red signal (PI staining). Scale bar = 50 μm.

Reference

1. Wang, J. H.; Liu, J. J.; Sümbelli, Y.; Shao, J. X.; Shi, X. Y.; van Hest, J. C. M. *J. Control. Release.* 2024, **372**, 59-68.
2. Cao, S. P.; Shao, J. X.; Wu, H. L.; Song, S. D.; De Martino, M. T.; Pijpers, I. A. B.; Friedrich, H.; Abdelmohsen, L. K. E. A.; Williams, D. S.; van Hest, J. C. M. *Nat. Commun.* 2021, **12,** 2077.
3. Wang, J. H.; Wu, H. L.; Zhu, X. W.; Zwolsman, R.; Hofstraat, S. R. J.; Li, Y. D.; Luo, Y. T.; Joosten, R. R. M.; Friedrich, H.; Cao, S. P.; et al. *Nat. Commun.* 2024, **15**, 4878.
4. Pijpers, I. A. B.; Abdelmohsen, L. K. E. A.; Williams, D. S.; van Hest, J. C. M. Morphology Under Control: Engineering Biodegradable Stomatocytes. *ACS Macro Lett.* 2017, **6**, 1217-1222.
5. Pijpers, I. A. B.; Cao, S. P.; Llopis-Lorente, A.; Zhu, J. Z.; Song, S. D.; Joosten, R. R. M.; Meng, F. H.; Friedrich, H.; Williams, D. S.; Sanchez, S.; et al. Hybrid Biodegradable Nanomotors through Compartmentalized Synthesis. *Nano Lett.* 2020, **20**, 4472-4480.
6. Luo, Y. T.; Wu, H. L.; Zhou, X.; Wang, J. H.; Er, S.; Li, Y. D.; Welzen, P. L. W.; Oerlemans, R. A. J. F.; Abdelmohsen, L. K. E. A.; Shao, J. X.; et al. *J. Am. Chem. Soc.* 2023, **145**, 20073-20080.
7. Wang, J. H.; Li, D.; Fan, Y.; Shi, M. H.; Yang, Y. X.; Wang, L.; Peng, Y. T.; Shen, M. W.; Shi, X. Y. *Nanoscale* 2019, **11**, 22343-22350.
8. Wang, J. H.; Luo, Y. T.; Wu, H. L.; Cao, S. P.; Abdelmohsen, L. K. E. A.; Shao, J. X.; van Hest, J. C. M. *Pharmaceutics* 2023, **15**, 1986.